FEBS Letters 584 (2010) 1615–1622

FEBS Letters

journal homepage: www.FEBSLetters.org

Decreased GLT-1 and increased SOD1 and HO-1 expression in astrocytes contribute to lumbar spinal cord vulnerability of SOD1-G93A transgenic mice

Yansu Guo [a,b,c], Weisong Duan [a,b,c], Zhongyao Li [a,b,c], Jing Huang [a,b,c], Yunxia Yin [a], Kunxi Zhang [a], Qian Wang [a], Zhifang Zhang [a], Chunyan Li [a,b,c,*]

[a] Department of Neurology, The Second Hospital of Hebei Medical University, Hebei, China
[b] Hebei Province Key Laboratory of Neurology, The Second Hospital of Hebei Medical University, Hebei, China
[c] Institute of Cardiocerebrovascular Disease, Hebei, China

ARTICLE INFO

Article history:
Received 10 February 2010
Revised 4 March 2010
Accepted 15 March 2010
Available online 18 March 2010

Edited by Jesus Avila

Keywords:
ALS
Astrocyte
SOD1
Heme oxygenase-1
Transgenic mice

ABSTRACT

The SOD1-G93A transgenic mouse is a widely used ALS model, but the death of lower motor neurons is the hallmark. Here, we show that the SOD1-G93A transgene and HO-1 are preferentially over-expressed in the lumbar spinal cord, particularly in the activated astrocytes of the transgenic mice. We also show down-regulation of GLT-1 in spite of the proliferating astrocytes. However, GLT-1, SOD1-G93A transgene and HO-1 expression were not obviously changed in the motor cortex. Our data link spinal cord vulnerability to relatively decreased expression of GLT-1, and high expression of the transgene and HO-1 in astrocytes in SOD1-G93A transgenic mice.

1. Introduction

Amyotrophic lateral sclerosis (ALS) is a progressively debilitating disease, causing selective loss of motor neurons from spinal cord, brainstem, and cortex, and results in paralysis and death. Approximately 5–10% of ALS cases are familial, 20% of which are caused by SOD1 mutations [1,2]. Transgenic mice expressing human SOD1-G93A replicate most phenotypes of human ALS, including weakness of hind limbs, loss of motor neurons, decreased glutamate uptake and formation of inclusions [2–4]. The pathogenesis of ALS likely involves multiple mechanisms, including excitotoxicity, oxidative stress and protein aggregation [5–7]. The exact mechanism of motor neuron degeneration remains undefined.

Motor neuron destruction in SOD1-G93A mice occurs primarily in the spinal cord, but the reason for spinal cord susceptibility is poorly understood. Mice expressing human SOD1-G93A develop astrocytosis in the spinal cord [8]. Significant loss of GLT-1 was previously reported in the spinal cord of SOD1-G85R transgenic mice [9] and SOD1-G93A transgenic rats [10]. However, conflicting data exist with respect to GLT-1 level in the spinal cord of SOD1-G93A transgenic mice [11,12]. In the present study, we compared the expression levels of both GFAP and GLT-1 in different central nervous system (CNS) parts in both SOD1-G93A mice and their non-transgenic littermates. Although, SOD1-G93A expression in transgenic rats was reported to increase in the spinal cord during the disease progression [10], the expression levels of SOD1-G93A in different CNS parts of transgenic mice are not well understood. Therefore, we have compared its expression levels in various CNS tissues. Moreover, oxidative stress has been increasingly implicated in the neurodegenerative process of ALS. Heme oxygenase-1 (HO-1) is a stress-responsive protein, whose expression is readily elevated in response to oxidative stress and injury. Using HO-1 as a biomarker of oxidative stress, we also compared the stress state of different CNS tissues in SOD1-G93A transgenic mice. At the same time, the cellular localization of SOD1 and HO-1 were analyzed using both immunohistochemistry and immunofluorescence. Our data provide important insight into the vulnerability of spinal cord in SOD1-G93A transgenic mice.

2. Materials and methods

2.1. Animals

Transgenic hSOD1-G93A mice and their non-transgenic littermates were generated by breeding male hemizygous carriers

* Corresponding author at: Department of Neurology, the Second Hospital of Hebei Medical University, 215 Heping Xi Road, Shijiazhuang, Hebei Province 050000, China. Fax: +86 311 87064024.
E-mail address: chunyanli5@yahoo.com.cn (C. Li).

0014-5793/$36.00 © 2010 Federation of European Biochemical Societies. Published by Elsevier B.V. All rights reserved.
doi:10.1016/j.febslet.2010.03.025

(B6SJL-Tg (SOD1-G93A) 1Gur/J) to female B6SJLF1 hybrids, both of which were purchased from the Jackson Laboratories (Bar Harbor, ME, USA). PCR-based genotyping of tail/blood DNA was used to identify the transgenic mice [2]. The animals were maintained in a 12-h light/dark cycle with ad libitum access to water and diet.

To monitor disease progression, the animals were inspected daily and weighed twice a week starting at 12 weeks of age. Disease onset was determined at the earliest presentation of gait abnormalities. When the animal could not upright itself in 30 s after being placed on either side or its back, it was scored as end stage [13]. After anesthesia with chloral hydrate (20 mg/mice), animals were sacrificed at pre-symptomatic stage (60 days of age), disease onset (100–120 days of age) or end stage (130–150 days of age), and the spinal cord, brain stem, hippocampus, cerebellum, and motor cortex were obtained for analysis. Experiments were carried out according to the regulations of laboratory animal management promulgated by the Ministry of Science and Technology of the People's Republic of China, which are in accordance with the guidelines published in the NIH Guide for the Care and Use of Laboratory Animals.

2.2. Immunoblotting analysis

Whole tissue extracts were prepared using a total protein extraction kit (Applygen Technologies Inc.) following the manufacturer's instruction. Protein levels in the extracts were quantified using the Bradford method. Forty micrograms of protein from each sample was run on 10% SDS–PAGE gels and blotted onto PVDF membranes. After probing the membranes with specific antibodies, including anti-β-actin, anti-SOD1 (Santa Cruz, CA, USA), and anti-HO-1 (StressGen Biotechnologies, Victoria, Canada), IRDye™ 700DX anti-mouse IgG, IRDye™ 800DX anti-rabbit IgG and IR Dye™ 800DX anti-goat IgG (Rockland, Maine, USA) were used and the bands of interest were detected using an Odyssey Infrared Imaging System (LI-COR, Lincoln, NE). Band intensity was quantified using the Odyssey Infrared Imaging System Version 2.1.12 and was normalized by the β-actin band. The original green or red color of a band was converted to black and white colors for data presentation.

2.3. Immunohistochemistry

After transcardial perfusion with 4% paraformaldehyde and further fixation for 24 h in the same fixative solution, lumbar enlargement was cut into 20 μm free-floating sections using a Leica VT 1000S vibratome. The sections were washed for three times in phosphate-buffered saline (PBS) and then perforated with 0.3% Triton X-100. After blocking with 3% H_2O_2 in methanol for 15 min and 10% horse serum for 1 h at room temperature, the sections were incubated overnight at 4 °C with antibodies against SOD1 (Santa Cruz, 1:200), and HO-1 (Stressgen Biotechnologies, 1:500), respectively. The sections were subsequently incubated with a biotin-conjugated secondary antibody (ZSGB-BIO, 1:200) for 2 h at room temperature, followed by incubation with HRP-conjugated streptavidin (ZSGB-BIO, 1:200) for 1 h at room temperature and treatment with 0.03% diaminobenzidine as a chromogen for 10 min. Slides were mounted and analyzed by light microscopy (Nikon 50i).

2.4. Confocal microscopy

The lumbar spinal cord fixed in 4% paraformaldehyde was cryoprotected in a 30% sucrose/4% paraformaldehyde solution for 12 h and then sliced into 30 μm sections using a Leica CM1850 freezing microtome. The sections were stained for HO-1 antibody in combination with anti-GFAP (Chemicon) or anti-SMI-32 (Sternberger) antibodies for double-labeling. Anti-SOD1 antibody in combination with anti-GFAP antibody was used for double-labeling. Fluorescent secondary antibodies (FITC conjugate of goat anti-rabbit, FITC conjugate of rabbit anti-goat and Cy5 conjugate of horse anti-mouse) were used. Slides were mounted and analyzed by fluorescent confocal microscopy (Olympus FV1000).

2.5. Reverse transcription-polymerase chain reaction (RT-PCR)

Human SOD1 mRNA levels from lumbar spinal cord and motor cortex of SOD1-G93A transgenic mice were evaluated by semi-quantitative RT-PCR, using GAPDH gene as internal standard. Total RNA was extracted from lumbar spinal cord and motor cortex at pre-symptomatic, onset and end stages of SOD1-G93A mice with Trizol reagent (Invitrogen Life Technologies, CA). cDNA was synthesized using M-MLV reverse transcriptase and random primers (Promega, WI). PCR primers specific to each gene are listed as follows: hSOD1, 5′-CAT CAG CCC TAA TCC ATC TGA-3′ and 5′-CGC GAC TAA CAA TCA AAG TGA-3′ (236-bp); GAPDH, 5′-ATG ACA TCA AGA AGG TGG TG-3′ and 5′-CAT ACC AGG AAA TGA GCT TG-3′ (177-bp). PCR was carried out in a 25 μl reaction volume and run for 35 cycles, using GoTaq® Green Master Mix from Promega. The amplification products were run in 2% agarose gel and stained with GoldView™ (Solarbio, Beijing, China). Quantitative analysis of RT-PCR results was performed by Gel-Pro Analyzer Version 3.0.

2.6. Statistical analysis

Results were expressed as means ± S.D. Statistical analyses were performed using one-way ANOVA followed by Student's *t*-test with SAS 8.0 statistical software. Differences were considered significant at $P < 0.05$.

3. Results

3.1. Differential expression of GFAP and GLT-1 in CNS tissues of non-transgenic littermates and time course of GFAP and GLT-1 expression in the lumbar spinal cord and cortex of SOD1-G93A transgenic mice

Since excitotoxicity is believed to play a significant role in the pathogenesis of motor neuron degeneration in ALS, and lumbar spinal cord is the main affected region in SOD1-G93A transgenic mice, we examined the expression of GFAP and GLT-1 in CNS tissues of the non-transgenic littermates. GFAP expression levels in the spinal cord and brain stem were similar but were significantly higher than that in the cerebellum, hippocampus and cortex. For example, GFAP level in the lumbar spinal cord was approximately twice as high as that in the cortex. In contrast, highest level of GLT-1 was detected in the cortex, which was approximately twofold higher than that in the spinal cord and brain stem (Fig. 1A). GLT-1 level in the cortex was approximately twice of that in the lumbar spinal cord. These results suggest that astrocytes in the spinal cord and brain stem may express relatively lower levels of GLT-1 and may be less capable of protecting against glutamate-mediated excitotoxicity than those in the brain cortex.

The expression levels of GFAP and GLT-1 in the lumbar spinal cord and motor cortex were measured at pre-symptomatic (60 days of age), disease onset (100–120 days of age) and end stages (130–150 days of age) of SOD1-G93A mice, as well as in their non-transgenic littermates (110–130 days of age). GLT-1 expression levels before and at disease onset in the lumbar spinal cord of the transgenic mice appeared to be somewhat higher than that in their littermates at the same age, but decreased significantly at the end stage. GFAP levels in the spinal cord of transgenic mice before disease onset was comparable to that in their littermates, but increased significantly at disease onset and increased

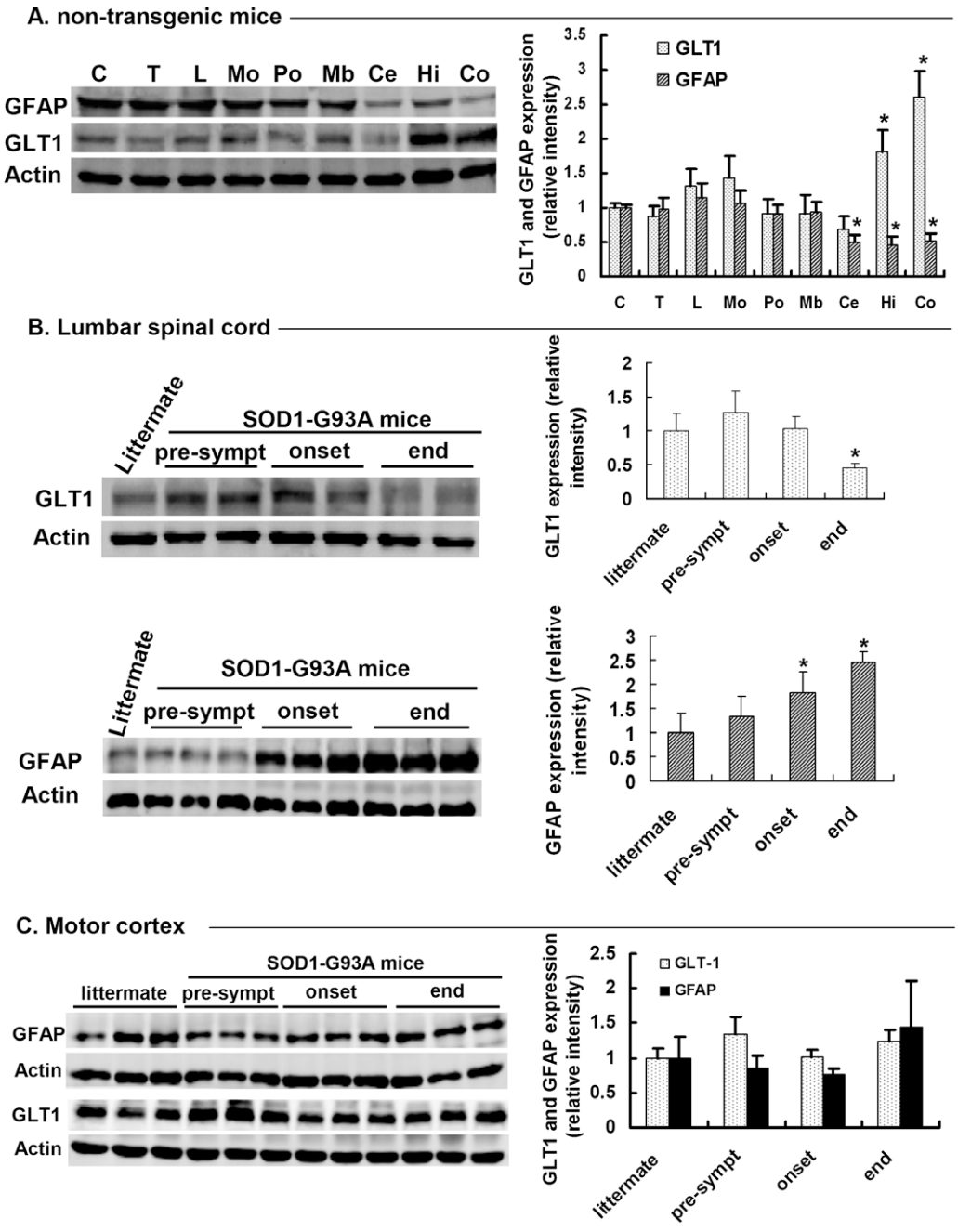

Fig. 1. Differential expression of GFAP and GLT-1 in CNS tissues of non-transgenic littermates and their changes with disease progression in lumbar spinal cord and motor cortex of SOD1-G93A transgenic mice. Total protein extracts from different CNS tissues of non-transgenic littermates at 110–130 days of age and SOD1-G93A transgenic mice at pre-symptomatic, onset and end stages were examined for levels of GFAP and GLT-1 by Western blot. β-Actin was used as a control. (A) GLT-1 is highly expressed in hippocampus and cortex, while GFAP expression is relative rich in the spinal cord and brain stem. $^*P < 0.05$ compared with the level in cervical spinal cord. (B) Time course of GFAP and GLT-1 expression in the lumbar spinal cord of SOD1-G93A transgenic mice. $^*P < 0.05$ compared with the level in the littermates. (C) Time course of GFAP and GLT-1 expression in the motor cortex of SOD1-G93A transgenic mice. No significant difference was found when compared with the littermates. The results are representative of triplicate experiments. C: cervical; T: thoracic; L: lumbar; Mo: Medulla oblongata; Po: pons; Mi: midbrain; Ce: cerebellum; Hi: hippocampus; Co: cortex. Pre-sympt: representative of pre-symptomatic stage.

further at the end stage (Fig. 1B). In contrast, neither GLT-1 nor GFAP expression in the cortex of the transgenic mice showed a time-related change and was similar to that in their littermates (Fig. 1C).

3.2. Differential expression of the SOD1-G93A transgene in CNS tissues of the transgenic mice

Expression of the human SOD1-G93A is the cause of motor neuron degeneration in SOD1-G93A transgenic mice. The SOD1 mutant is presumably expressed in all types of cells and tissues in the mice. However, its expression level differed significantly among spinal cord and other CNS tissues at as early as 60 days of age in SOD1-G93A transgenic mice. Its expression was markedly higher in the spinal cord than in other tissues (Fig. 2A). Its level in the lumbar spinal cord was the highest, which was approximately sixfold higher than in the cortex at the end stage. Similarly, wild type hSOD1 transgenic mice also had higher expression of human SOD1 in the lumbar spinal cord (about fourfold hither) than in the cortex (Fig. 2B). Moreover, the SOD1-G93A protein in the

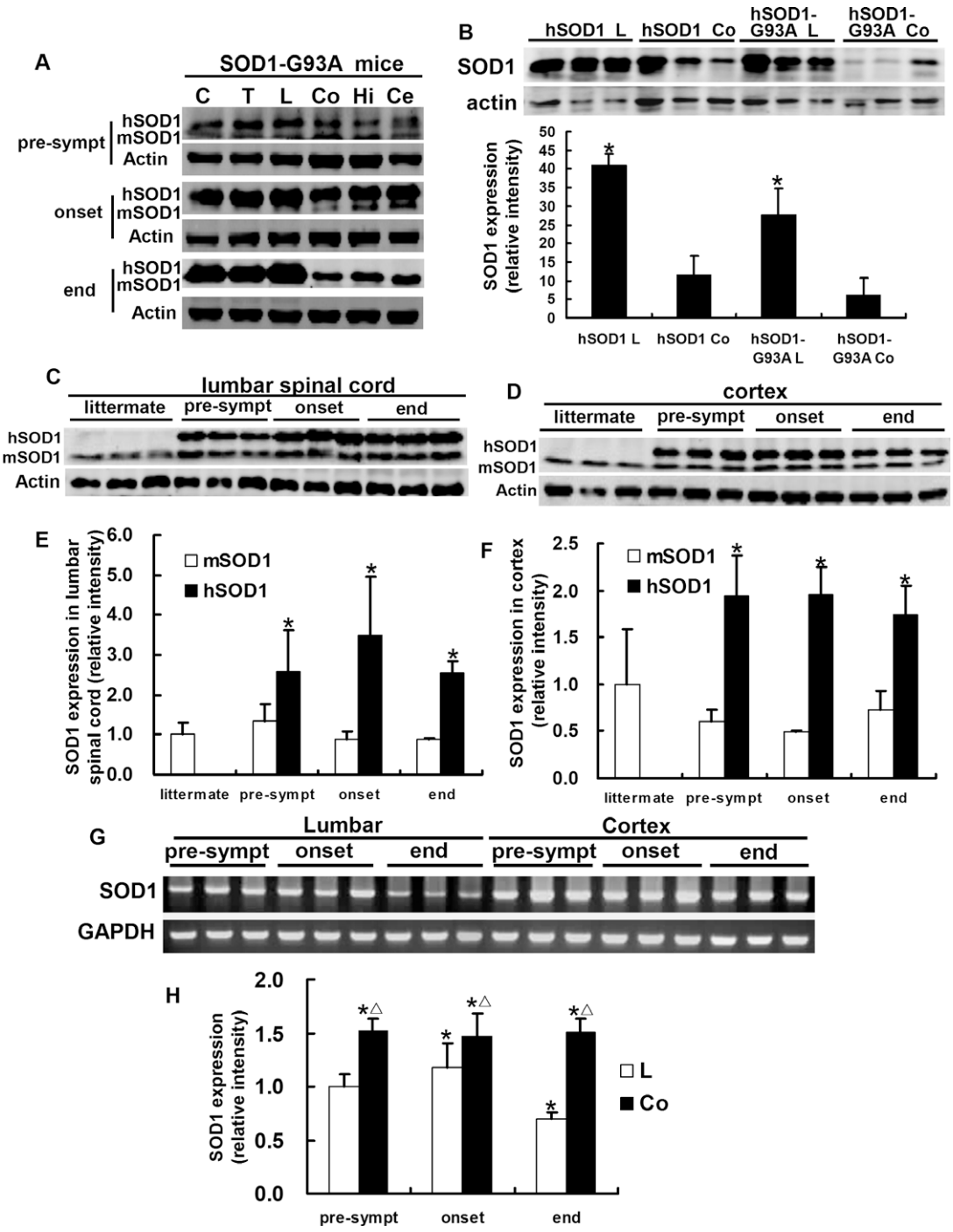

Fig. 2. Increased protein expression and decreased mRNA level of the SOD1-G93A transgene in the lumbar spinal cord at end stage of SOD1-G93A transgenic mice. Different CNS tissues were harvested from non-transgenic littermates (110–130 days of age) and transgenic mice at pre-symptomatic stage, disease onset or end stage, respectively. Crude tissue extracts were examined for SOD1 expression by Western blot, using β-actin as a control. (A) The expression of SOD1-G93A transgene in the spinal cord was higher than any other CNS tissues at different disease stages. (B) Total SOD1 expression in lumbar spinal cord and motor cortex of hSOD1-G93A transgenic mice at end stage and wild type hSOD1 transgenic mice at the same age. $^{*}P < 0.05$ compared with motor cortex of the same transgenic mice. (C and D) Time course of SOD1-G93A transgene expression in the lumbar spinal cord and motor cortex of the transgenic mice. (E and F) Histograms of SOD1 expression in C and D, respectively. $^{*}P < 0.05$ compared with mouse SOD1 expression in non-transgenic littermates. (G) Time course of human SOD1 mRNA levels in the lumbar spinal cord and motor cortex of SOD1-G93A transgenic mice. (H) Histograms of SOD1 expression in G. $^{*}P < 0.05$ compared with pre-symptomatic L; Δ, compared with end L. The results are representative of triplicate experiments. Pre-sympt, representative of pre-symptomatic stage. C: cervical; T: thoracic; L: lumbar; Co: motor cortex; Hi: hippocampus; Ce: cerebellum. hSOD1: human SOD1; mSOD1: mouse SOD1.

lumbar spinal cord tissue appeared to increase as the disease progressed (Fig. 2C and E). However, the expression of SOD1 mutant in the motor cortex of SOD1-G93A transgenic mice did not change significantly at different disease stages (Fig. 2D and F). In order to further explore the reason why lumbar spinal cord had more SOD1 mutant proteins, we performed RT-PCR analysis on human SOD1 in lumbar spinal cord and motor cortex of SOD1-G93A transgenic mice at different stages. Interestingly, the human SOD1 mRNA level showed constantly higher (about 1.5 fold higher than lumbar spinal cord) in the motor cortex, while it increased at dis-

ease onset and decreased significantly at the end stage in the lumbar spinal cord of SOD1-G93A transgenic mice (Fig. 2G and H).

3.3. Proliferated astrocytes expressed SOD1 in the lumbar spinal cord of symptomatic SOD1-G93A transgenic mice

We also observed that as the disease progressed, GFAP-positive astrocytes increased and motor neurons decreased progressively (data not shown). To determine the cellular localization of SOD1, we performed double-labeling fluorescent confocal microscopy, detecting both SOD1 and GFAP. Low SOD1 and GFAP expression were detected in the lumbar spinal cord of the non-transgenic littermates, with SOD1 mainly expressed in neurons and astrocytes and GFAP expressed in astrocytes. However, their expression levels were very high at disease onset in the transgenic mice (Fig. 3A), which is consistent with the Western blot results shown in Fig. 2. Moreover, except for SOD1-positive remanent neurons, SOD1 expression co-localized nicely with GFAP-positive astrocytes in the lumbar spinal cord of the transgenic mice at disease onset (Fig. 3A). These results suggest that the SOD1-G93A transgene is over-expressed in both the proliferating astrocytes and neurons in the lumbar spinal cord of SOD1-G93A transgenic mice. In con-

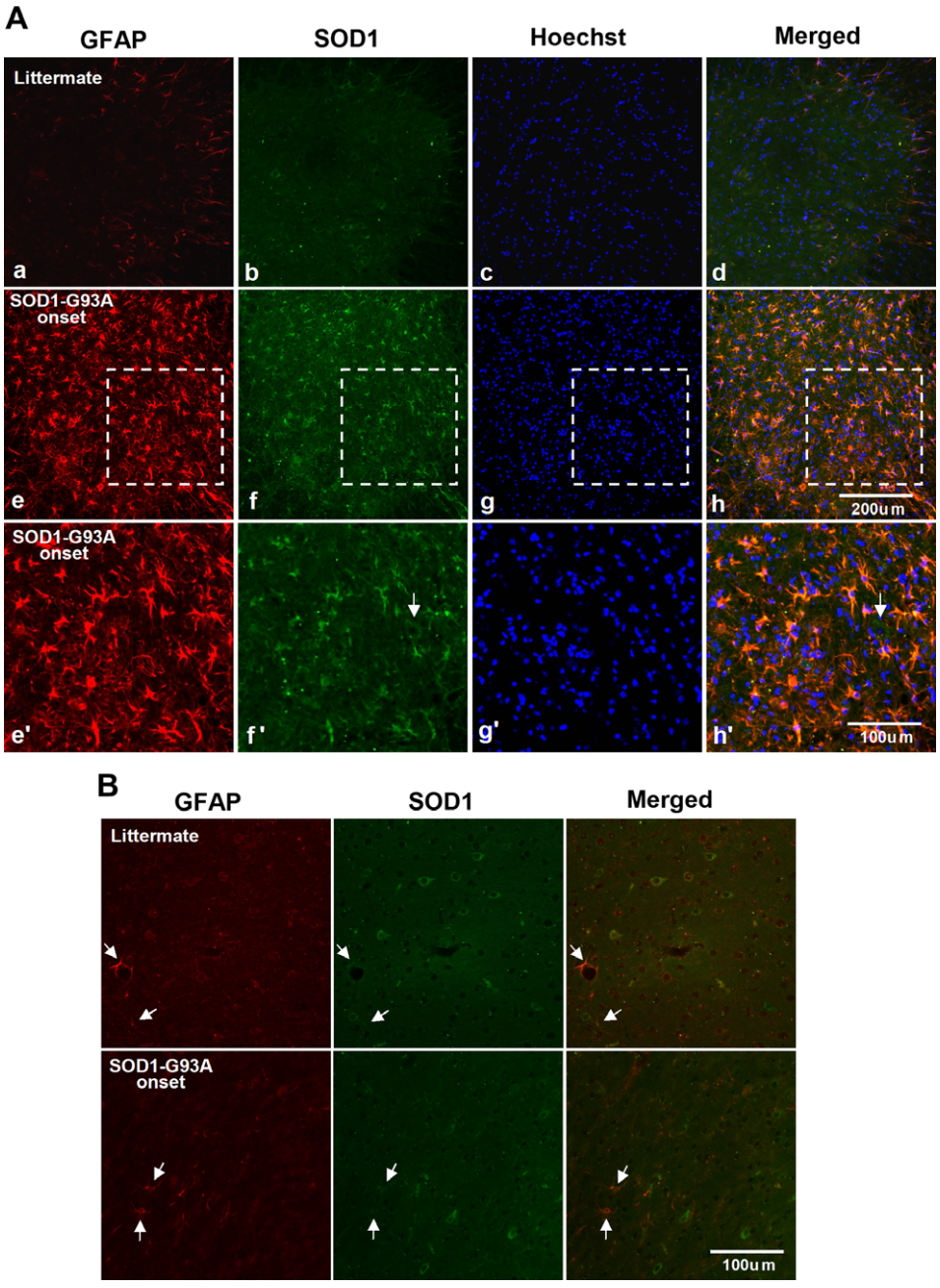

Fig. 3. Cellular localization of SOD1-G93A transgene in the lumbar spinal cord and motor cortex of symptomatic SOD1-G93A transgenic mice and non-transgenic littermates. Tissue sections of lumbar spinal cord and motor cortex of the transgenic mice at onset stage and their littermates at the same age were subjected to GFAP and SOD1 double-labeling fluorescent confocal microscopy. (A) GFAP and SOD1 expression was low in the lumbar spinal cord of non-transgenic littermates (a–d), but markedly increased in the transgenic mice at the onset stage (e–h) and SOD1 expression co-localized with GFAP expression nicely (e′–h′). GFAP was used to locate astrocytes. Nuclei were labeled with Hoechst. Arrow: a SOD1-positive remanent neuron. (e′–h′) were enlargements of the dotted areas in (e–h), respectively. (a–h) Bar = 200 μm. (e′–h′) Bar = 100 μm. (B) GFAP-positive astrocytes did not proliferate or over-express SOD1 compared with non-transgenic littermates in the motor cortex (arrows indicate astrocytes). Neurons were SOD1-positive. Bar = 100 μm.

trast, GFAP-positive astrocytes in the motor cortex of SOD1-G93A mice did not proliferate and expressed low SOD1 level (Fig. 3B). Using immunohistochemistry, we observed low basal SOD1 expression in both cytoplasm and nucleus of neurons in the lumbar spinal cord of non-transgenic littermates. However, in SOD1-G93A transgenic mice, much higher intensity of SOD1 expression was found at any disease stages including 60 days, onset and end stages. Notably, many dark-brown SOD1-positive motor neurons were noticed in the lumbar anterior horn of SOD1-G93A transgenic mice at 60 days of age. Besides, some astrocyte-like SOD1-positive cells were also observed, which was in accordance with the results of confocal microscopy (Supplementary Fig. 1).

3.4. Different HO-1 reactivity in the CNS and HO-1 cellular localization in the lumbar spinal cord of SOD1-G93A transgenic mice

HO-1 expression levels were relatively low in the CNS tissues of non-transgenic littermates and did not show significant change over the time course. Therefore, littermates at 110–130 days were used as non-transgenic control in the Western blot analysis. HO-1 expression level was low in SOD1-G93A transgenic mice at 60 days of age, similar to their littermates. However, its level in the spinal cord of the transgenic mice, particularly in the lumbar spinal cord, increased significantly at disease onset and end stages. In contrast, HO-1 levels in motor cortex of the transgenic mice were not changed significantly with the disease progression (Fig. 4).

To determine the cellular localization of HO-1, we performed double-labeled fluorescent confocal microscopy (Supplementary Fig. 2). HO-1 expression was barely detectable in the cytoplasm of neurons in the lumbar spinal cord of non-transgenic littermates, but readily detected in the lumbar spinal cord of the transgenic mice at disease onset. Some of the remanent neurons were strongly HO-1 positive, showing clear cytoplasmic staining, consistent with the known cellular location of HO-1. Most of the HO-1-positive cells were astrocytes, based on the co-localization of HO-1 and GFAP. We further performed HO-1 immunohistochemistry, and achieved the same results as confocal microscopy did. HO-1 was low-expressed mainly in the cytoplasm of neurons in the lumbar spinal cord of non-transgenic littermates. The intensity of HO-1 immunoreactivity increased in SOD1-G93A transgenic mice.

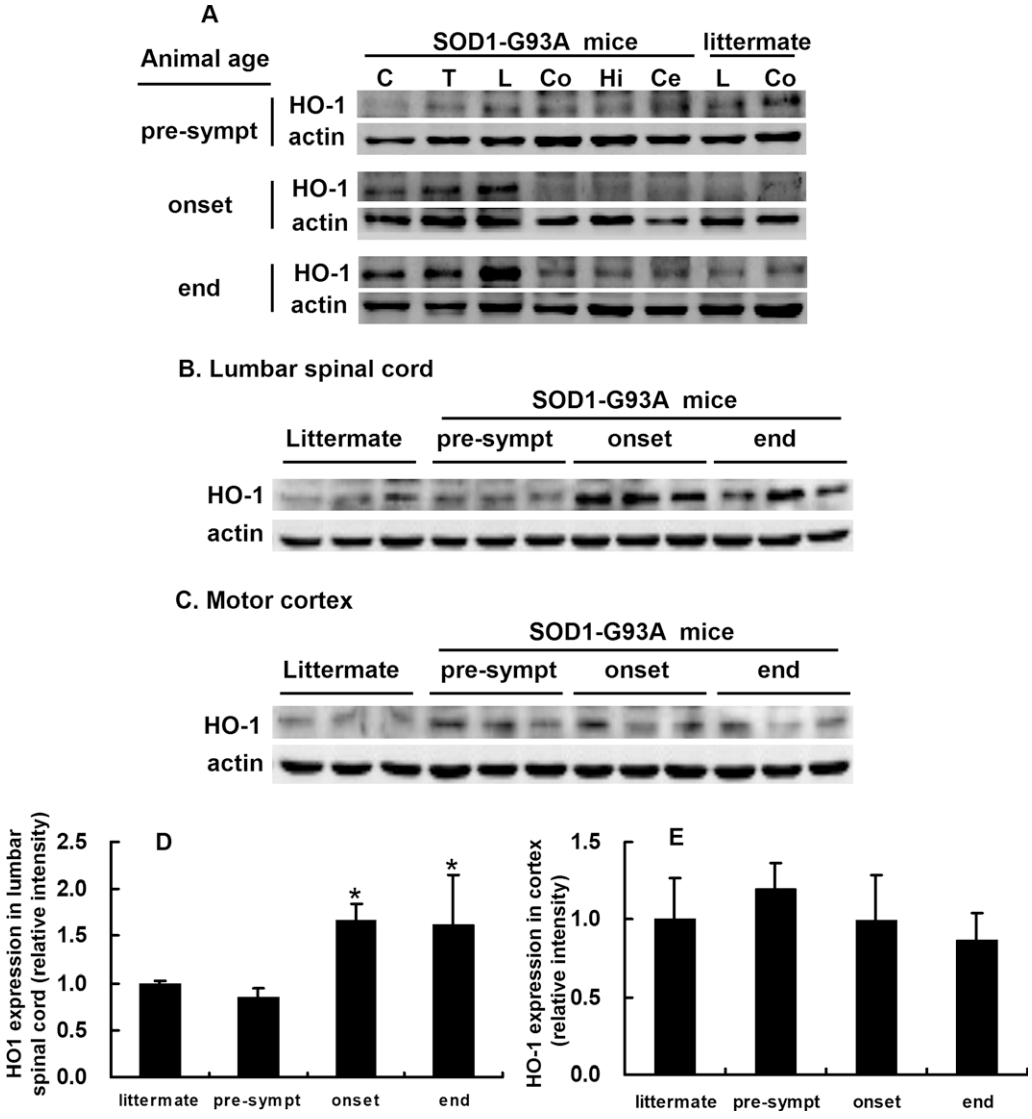

Fig. 4. Time course of HO-1 expression in CNS tissues of SOD1-G93A transgenic mice. (A) HO-1 levels in various CNS tissues of SOD1-G93A transgenic mice at pre-symptomatic stage, disease onset or end stage and their non-transgenic littermates at the same ages were measured by Western blot. (B and C) HO-1 expression levels in the lumbar spinal cord and motor cortex of the transgenic mice at different stages and their non-transgenic littermates at 110–130 days of age. (D and E) Histograms of HO-1 expression in (B and C), respectively. $^{*}P < 0.05$ compared with non-transgenic littermates. Pre-sympt, representative of pre-symptomatic stage.

Importantly, some HO-1 strongly positive astrocyte-like cells appeared in the lumbar anterior horn nearby motor neurons at 60 days of age and increased and hypertrophied with the disease progression, which was in accordance with the results found in confocal microscopic examination. These proliferated HO-1 positive astrocyte-like cells were not detected in the lumbar dorsal horn. Meanwhile, some individual HO-1 strongly positive neurons were also observed as in the confocal microscopic photographs (Supplementary Fig. 3).

4. Discussion

To the best of our knowledge, this is the first time that differential expression of human SOD1 transgene has been shown in the CNS tissues of SOD1-G93A transgenic mice. The expression of SOD1-G93A transgene was significantly higher in the spinal cord than in the brainstem, cerebellum, hippocampus and cortex. Moreover, in the lumbar spinal cord, the expression of this transgene increased as the disease progressed. However, similar difference was found on wild type human SOD1 transgene expression between lumbar spinal cord and motor cortex of human SOD1 transgenic mice. Therefore, the relatively high expression of mutant human SOD1 is not the only reason contributed to the vulnerability of spinal cord in SOD1-G93A mice. Our RT-PCR results further showed that the SOD1-G93A transgene mRNA level in lumbar spinal cord was much lower than that in motor cortex of SOD1-G93A transgenic mice. Thus, we speculate that there may be a disturbance of mutant SOD1 degradation in the lumbar spinal cord, while the over-expressed wild type hSOD1 in the lumbar spinal cord could be properly degraded and did not cause toxic injury to motor neurons. We also showed that SOD1-G93A transgene was mainly expressed in motor neurons forming aggregations at presymptomatic stage (60 days of age), and with the disease progression, astrocytes proliferated and over-expressed SOD1-G93A protein. SOD1-G93A expressing astrocytes are toxic to motor neurons by releasing unidentified molecules in vitro [14] and enhance microglial activation [15]. Therefore, SOD1-G93A expressing astrocytes could be accelerator of motor neuron death and disease progression and contribute to spinal cord vulnerability.

GLT-1, which is predominantly astroglial, is known to play a crucial role in maintaining a normal extracellular glutamate level. Our present study showed that tissue levels of GLT-1 differed among different CNS tissues in non-transgenic littermate mice. Its level in the spinal cord, particularly after adjustment by GFAP expression, was similar to those in medulla oblongata, pons, but much lower than that in hippocampus and cortex. It has been widely shown that astrocytes become reactive in ALS transgenic mice, known as reactive gliosis. Increase of astrocyte number and hypertrophy of astrocyte processes are two hallmarks of reactive gliosis, which would resulted in upregulation of its cytoskeleton known as GFAP [16]. We further observed a progressively increased level of GFAP protein, accompanied by decreased GLT-1 protein levels in the lumbar spinal cord of SOD1-G93A mice, but no changes of GFAP and GLT-1 were detected in the cortex of these animals. Several studies have documented a loss of GLT-1 in ALS patients [17,18], SOD1-G93A transgenic rat [10] and SOD1-G93A transgenic mice [11]. Indeed, in vitro studies showed that the toxic effect of SOD1-G93A could cause a specific post-translational down regulation of GLT-1 by increasing the removal of the transporter from the cell surface and targeting the internalized transporter for degradation [19]. In our study, spinal cord changes of GLT1 and GFAP appear to follow SOD1-G93A transgene expression, since the expression level of neither GLT1 nor GFAP in the SOD1-G93A spinal cord at 60 days of age was different from that in the littermates, while SOD1-G93A transgene significantly over-expressed at that time.

HO-1 is sensitive to oxidative stress and is up-regulated in response to a wide variety of stimuli, including hypoxia, depletion of reduced glutathione, nitric oxide and others [20–23]. Up regulation of HO-1 may confer protection against oxidative insults both in vitro [24,25] and in vivo [26,27]. HO-1 induction has been reported in SOD1-G93A transgenic rats [28] and other neurodegenerative diseases, such as AD and PD [29,30]. In this study, HO-1 was used as a marker of oxidative stress, although up-regulation of HO-1 may also enhance cytoprotection. Its expression was significantly induced in the spinal cord in a time-dependent manner in SOD1-G93A mice, reaching maximal levels at the end stage, whereas no significant HO-1 induction was observed in the other CNS tissues. HO-1 immunoreactivity was increased in the lumbar anterior horn of SOD1-G93A mice and characteristically co-localized with GFAP. These results suggest that the reactive astrocytes in the spinal cord are under significant oxidative stress. However, HO1 induction in the spinal cord was secondary to SOD1-G93A expression, as the latter gene was already highly expressed at 60 days of age, when no induction of HO-1 had yet occurred.

In conclusions, spinal cord vulnerability in human SOD1-G93A transgenic mice is closely correlated with activated astrocytes expressing high levels of SOD1-G93A transgene and HO-1 and low level of GLT-1. ALS therapies aimed at these aspects will be prospective.

Acknowledgements

This study was supported in part by grants from Natural Science Foundation of China (30670732; 30870882; 30900460) and a grant from Science and Technological department of Hebei Province (08966105D). We thank Yongbo Sui for his technical supports.

Appendix A. Supplementary data

Supplementary data associated with this article can be found, in the online version, at doi:10.1016/j.febslet.2010.03.025.

References

[1] Rosen, D.R., Siddique, T., Patterson, D., Figlewicz, D.A., Sapp, P., Hentati, A., Donaldson, D., Goto, J., O'Regan, J.P., Deng, H.X., et al. (1993) Mutations in Cu/Zn superoxide dismutase gene are associated with familial amyotrophic lateral sclerosis. Nature 362, 59–62.
[2] Gurney, M.E., Pu, H., Chiu, A.Y., Dal Canto, M.C., Polchow, C.Y., Alexander, D.D., Caliendo, J., Hentati, A., Kwon, Y.W., Deng, H.X., et al. (1994) Motor neuron degeneration in mice that express a human Cu, Zn superoxide dismutase mutation. Science 264, 1772–1775.
[3] Canton, T., Pratt, J., Stutzmann, J.M., Imperato, A. and Boireau, A. (1998) Glutamate uptake is decreased tardively in the spinal cord of FALS mice. Neuroreport 9, 775–778.
[4] Watanabe, M., Dykes-Hoberg, M., Culotta, V.C., Price, D.L., Wong, P.C. and Rothstein, J.D. (2001) Histological evidence of protein aggregation in mutant SOD1 transgenic mice and in amyotrophic lateral sclerosis neural tissues. Neurobiol. Dis. 8, 933–941.
[5] Carrí, M.T., Ferri, A., Cozzolino, M., Calabrese, L. and Rotilio, G. (2003) Neurodegeneration in amyotrophic lateral sclerosis: the role of oxidative stress and altered homeostasis of metals. Brain Res. Bull. 61, 365–374.
[6] Rothstein, J.D. (1995) Excitotoxicity and neurodegeneration in amyotrophic lateral sclerosis. Clin. Neurosci. 3, 348–359.
[7] Julien, J.P. (1995) A role for neurofilaments in the pathogenesis of amyotrophic lateral sclerosis. Biochem. Cell Biol. 73, 593–597.
[8] Hall, E.D., Oostveen, J.A. and Gurney, M.E. (1998) Relationship of microglial and astrocytic activation to disease onset and progression in a transgenic model of familial ALS. Glia 23, 249–256.
[9] Bruijn, L.I., Becher, M.W., Lee, M.K., Anderson, K.L., Jenkins, N.A., Copeland, N.G., Sisodia, S.S., Rothstein, J.D., Borchelt, D.R., Price, D.L. and Cleveland, D.W. (1997) ALS-linked SOD1 mutant G85R mediates damage to astrocytes and promotes rapidly progressive disease with SOD1-containing inclusions. Neuron 18, 327–338.
[10] Howland, D.S., Liu, J., She, Y., Goad, B., Maragakis, N.J., Kim, B., Erickson, J., Kulik, J., DeVito, L., Psaltis, G., DeGennaro, L.J., Cleveland, D.W. and Rothstein, J.D. (2002) Focal loss of the glutamate transporter EAAT2 in a transgenic rat model of SOD1 mutant mediated amyotrophic lateral sclerosis (ALS). Proc. Natl. Acad. Sci. USA 99, 1604–1609.

[11] Bendotti, C., Tortarolo, M., Suchak, S.K., Calvaresi, N., Carvelli, L., Bastone, A., Rizzi, M., Rattray, M. and Mennini, T. (2001) Transgenic SOD1 G93A mice develop reduced GLT-1 in spinal cord without alterations in cerebrospinal fluid glutamate levels. J. Neurochem. 79, 737–746.
[12] Sasaki, S., Warita, H., Abe, K., Komori, T. and Iwata, M. (2001) EAAT1 and EAAT2 immunoreactivity in transgenic mice with a G93A mutant SOD1 gene. Neuroreport 12, 1359–1362.
[13] Weydt, P., Hong, S.Y., Kliot, M. and Moller, T. (2003) Assessing disease onset and progression in the SOD1 mouse model of ALS. Neuroreport 14, 1051–1054.
[14] Nagai, M., Re, D.B., Nagata, T., Chalazonitis, A., Jessell, T.M., Wichterle, H. and Przedborski, S. (2007) Astrocytes expressing ALS-linked mutated SOD1 release factors selectively toxic to motor neurons. Nat. Neurosci. 10, 615–622.
[15] Yamanaka, K., Chun, S.J., Boillee, S., Fujimori-Tonou, N., Yamashita, H., Gutmann, D.H., Takahashi, R., Misawa, H. and Cleveland, D.W. (2008) Astrocytes as determinants of disease progression in inherited amyotrophic lateral sclerosis. Nat. Neurosci. 11, 251–253.
[16] Pekny, M. and Pekna, M. (2004) Astrocyte intermediate filaments in CNS pathologies and regeneration. J. Pathol. 204, 428–437.
[17] Rothstein, J.D., van Kammen, M., Levy, A.I., Martin, L.J. and Kuncl, R.W. (1995) Selective loss of glial glutamate transporter GLT-1 in amyotrophic lateral sclerosis. Ann. Neurol. 38, 73–84.
[18] Bristol, L.A. and Rothstein, J.D. (1996) Glutamate transporter gene expression in amyotrophic lateral sclerosis motor cortex. Ann. Neurol. 39, 676–679.
[19] Vanoni, C., Massari, S., Losa, M., Carrega, P., Perego, C., Conforti, L. and Pietrini, G. (2004) Increased internalisation and degradation of GLT-1 glial glutamate transporter in a cell model for familial amyotrophic lateral sclerosis (ALS). J. Cell Sci. 117, 5417–5426.
[20] Choi, A.M. and Alam, J. (1996) Heme oxygenase-1: function, regulation, and implication of a novel stress-inducible protein in oxidant-induced lung injury. Am. J. Respir. Cell Mol. Biol. 15, 9–19.
[21] Lee, P.J., Alam, J., Sylvester, S.L., Inamdar, N., Otterbein, L. and Choi, A.M. (1996) Regulation of heme oxygenase-1 expression in vivo and in vitro in hyperoxic lung injury. Am. J. Respir. Cell Mol. Biol. 14, 556–568.
[22] Horikawa, S., Yoneya, R., Nagashima, Y., Hagiwara, K. and Ozasa, H. (2002) Prior induction of heme oxygenase-1 with glutathione depletor ameliorates the renal ischemia and reperfusion injury in the rat. FEBS Lett. 510, 221–224.
[23] Foresti, R., Clark, J.E., Green, C.J. and Motterlini, R. (1997) Thiol compounds interact with nitric oxide in regulating heme oxygenase-1 induction in endothelial cells: involvement of superoxide and peroxynitrite anions. J. Biol. Chem. 272, 18411–18417.
[24] Gong, P., Cederbaum, A.I. and Nieto, N. (2004) Heme oxygenase-1 protects HepG2 cells against cytochrome P450 2E1-dependent toxicity. Free Radic. Biol. Med. 36, 307–318.
[25] Abraham, N.G., Kushida, T., McClung, J., Weiss, M., Quan, S., Lafaro, R., Darzynkiewicz, Z. and Wolin, M. (2003) Heme oxygenase-1 attenuates glucose-mediated cell growth arrest and apoptosis in human microvessel endothelial cells. Circ. Res. 93, 507–514.
[26] Fujii, H., Takahashi, T., Nakahira, K., Uehara, K., Shimizu, H., Matsumi, M., Morita, K., Hirakawa, M., Akagi, R. and Sassa, S. (2003) Protective role of heme oxygenase-1 in the intestinal tissue injury in an experimental model of sepsis. Crit. Care Med. 31, 893–902.
[27] Otterbein, L., Sylvester, S.L. and Choi, A.M. (1995) Hemoglobin provides protection against lethal endotoxemia in rats: the role of heme oxygenase-1. Am. J. Respir. Cell Mol. Biol. 13, 595–601.
[28] Vargas, M.R., Pehar, M., Cassina, P., Martínez-Palma, L., Thompson, J.A., Beckman, J.S. and Barbeito, L. (2005) Fibroblast growth factor-1 induces heme oxygenase-1 via nuclear factor erythroid 2-related factor 2 (Nrf2) in spinal cord astrocytes: consequences for motor neuron survival. J. Biol. Chem. 280, 25571–25579.
[29] Takeda, A., Itoyama, Y., Kimpara, T., Zhu, X., Avila, J., Dwyer, B.E., Perry, G. and Smith, M.A. (2004) Heme catabolism and heme oxygenase in neurodegenerative disease. Antioxid. Redox Signal. 6, 888–894.
[30] Schipper, H.M. (2004) Heme oxygenase expression in human central nervous system disorders. Free Radic. Biol. Med. 37, 1995–2011.